





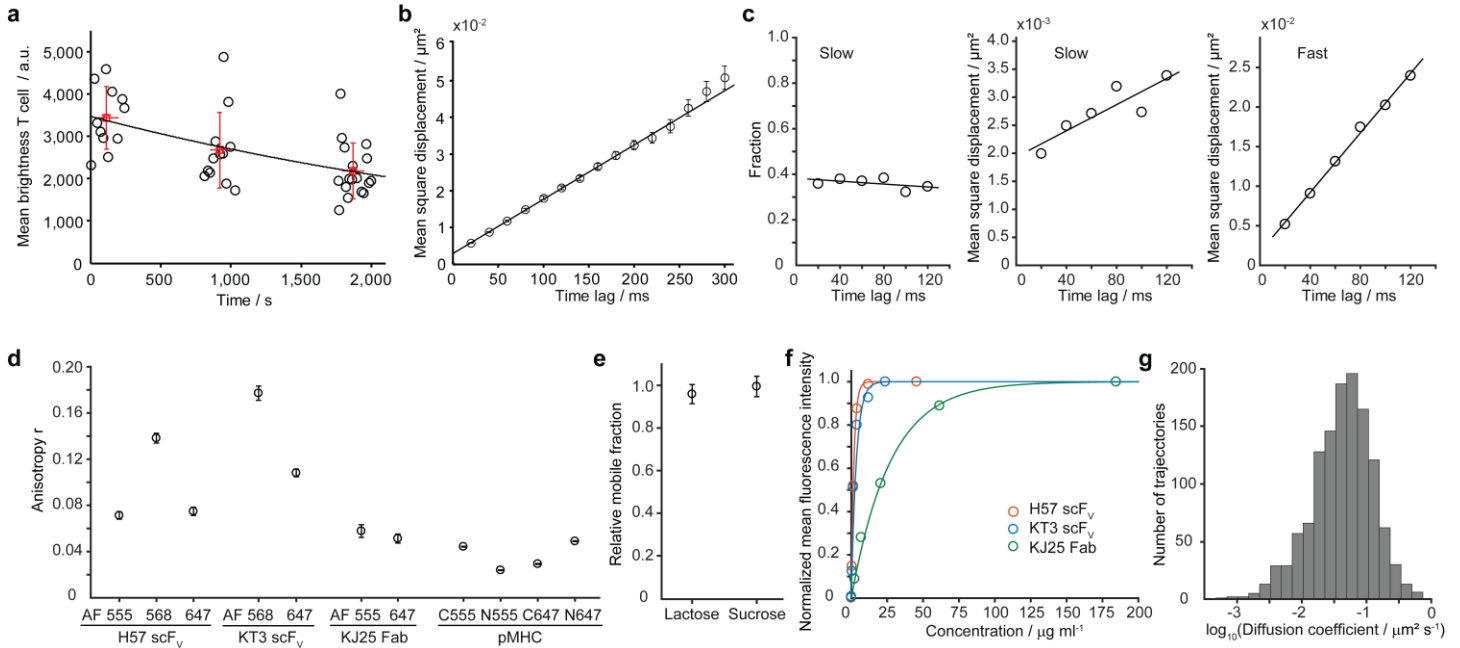


In the format provided by the authors and unedited.

Monomeric TCRs drive T cell antigen recognition

Mario Brameshuber ^{1*}, Florian Kellner ^{2,7}, Benedikt K. Rossboth ^{1,7}, Haisen Ta³, Kevin Alge²,
Eva Sevcsik¹, Janett Göhring^{1,2}, Markus Axmann⁴, Florian Baumgart¹, Nicholas R. J. Gascoigne ⁵,
Simon J. Davis⁶, Hannes Stockinger ², Gerhard J. Schütz¹ and Johannes B. Huppa ^{2*}

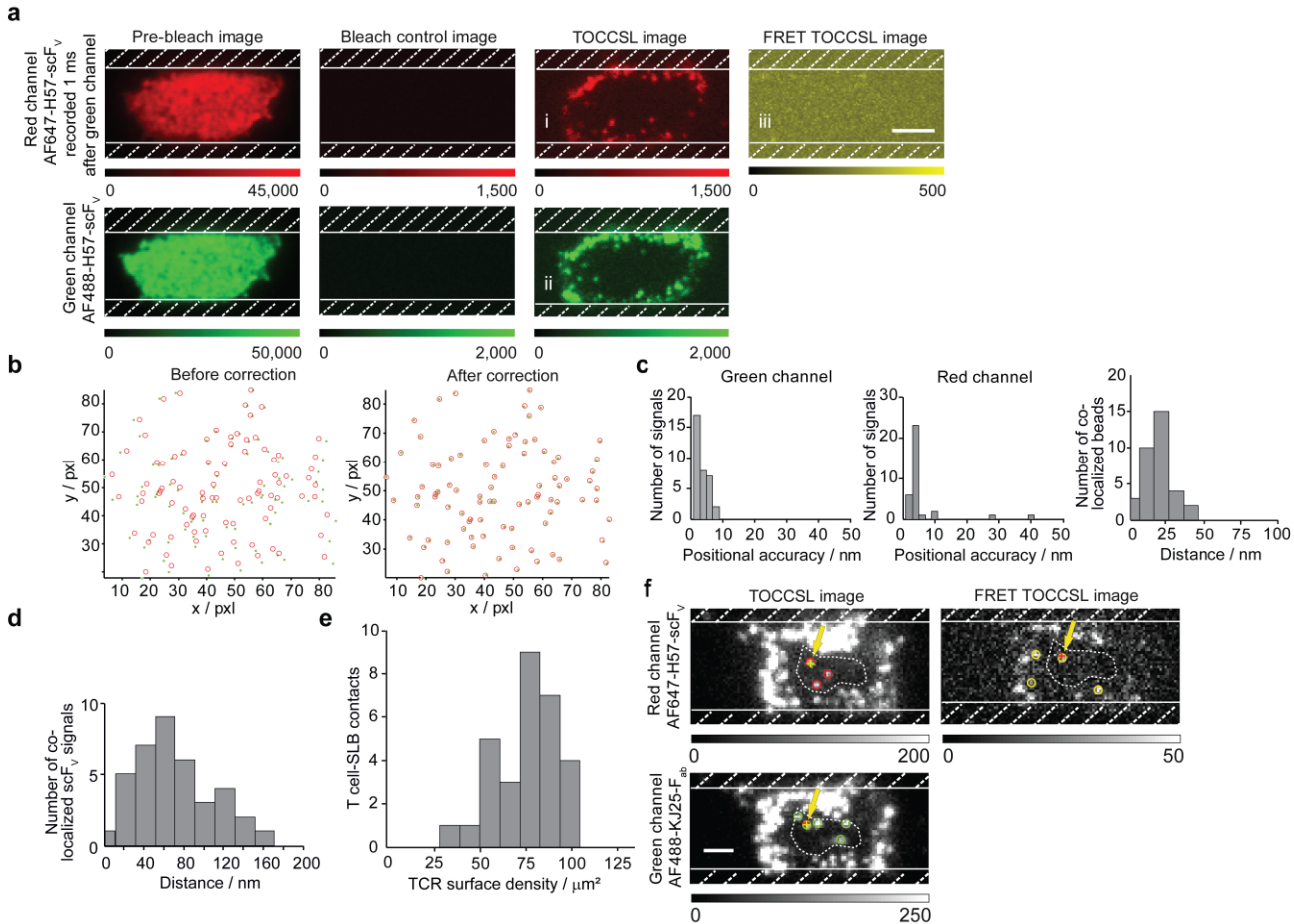
¹Institute of Applied Physics, TU Wien, Vienna, Austria. ²Center for Pathophysiology, Infectiology and Immunology, Institute for Hygiene and Applied Immunology, Medical University of Vienna, Vienna, Austria. ³Department of NanoBiophotonics, Max Planck Institute for Biophysical Chemistry, Göttingen, Germany. ⁴Center for Pathobiochemistry and Genetics, Institute of Medical Chemistry and Pathobiochemistry, Medical University of Vienna, Vienna, Austria. ⁵Department of Microbiology and Immunology, Yong Loo Lin School of Medicine, National University of Singapore, Singapore, Singapore. ⁶Radcliffe Department of Medicine and MRC Human Immunology Unit, John Radcliffe Hospital, University of Oxford, Oxford, UK. ⁷These authors contributed equally: Florian Kellner and Benedikt K. Rossboth. *e-mail: brameshuber@iap.tuwien.ac.at; johannes.huppa@meduniwien.ac.at



Supplementary Figure 1

Analysis of H57-scFv binding lifetime, TCR diffusion, anisotropy, TCR diffusion under lactose treatment, target binding of antibody probes and distribution of TCR diffusion constants

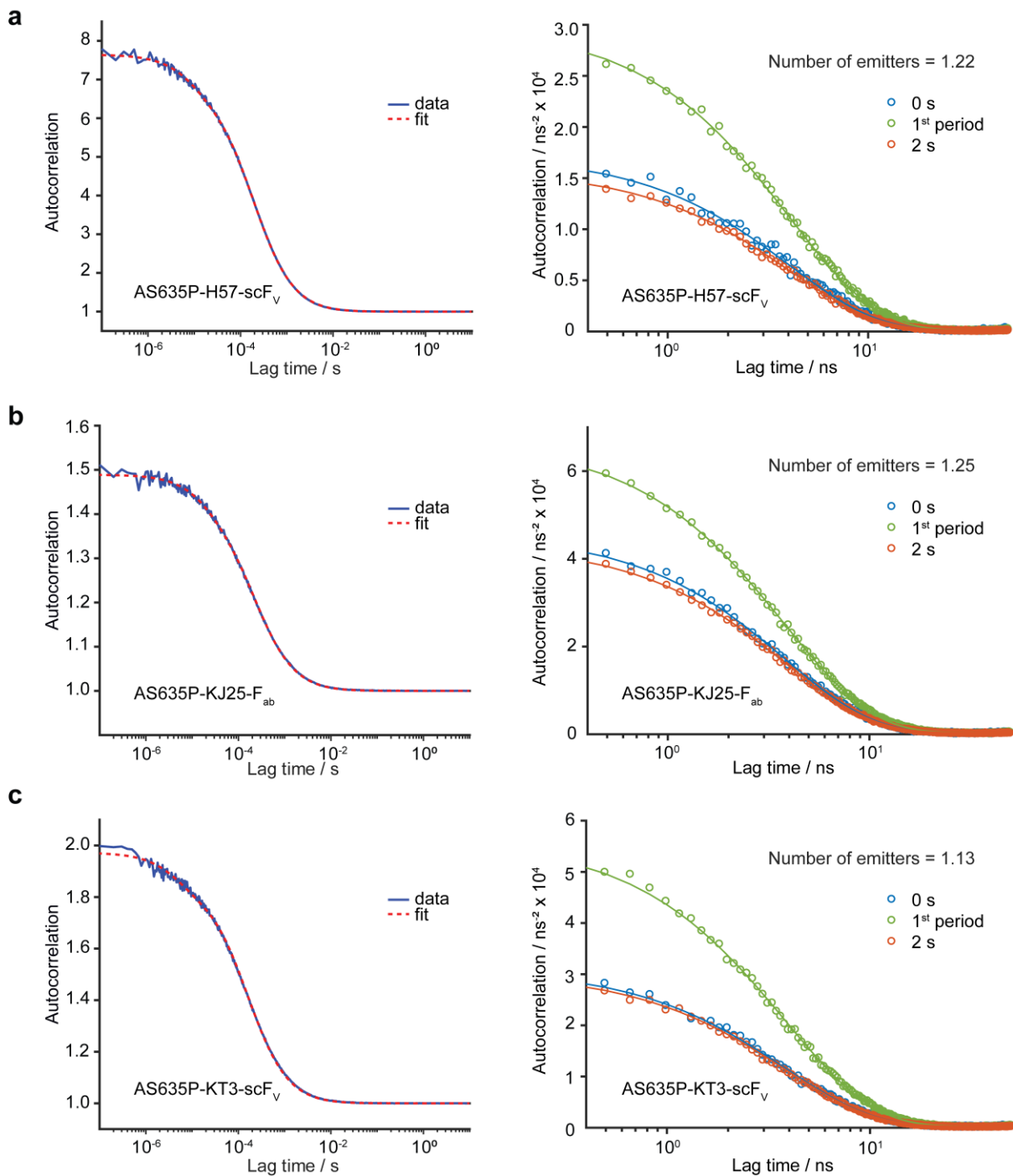
a, The half-life of AF647-H57-scFv bound to surface-exposed TCRs was determined as follows: T cells were labeled under saturating conditions with AF647-H57-scFv and placed onto a lipid bilayer featuring the adhesion molecule ICAM-1. The background-subtracted mean brightness values of individual T cells were determined in TIR mode at various time points (black open circles). Acquired intensities were determined for three time intervals, 0–200 s ($n = 11$ cells), 800–1,050 s ($n = 12$ cells) and 1,750–2,000 s ($n = 17$ cells), and average values were calculated (red open square). The resulting curve was fitted to a single-exponential function and yielded a half-life $t_{1/2}$, of 44 ± 9 min at room temperature. **b**, TCR diffusion constants were determined as follows: TCRs were labeled with AF647-H57-scFv and single-molecule tracking experiments were performed. Mean square displacements were determined and are plotted as a function of time lags. Assuming pure Brownian motion, a linear fit yielded a diffusion coefficient D of $0.037 \pm 0.002 \mu\text{m}^2/\text{s}$ ($n = 21$ cells). **c**, The immobile fraction of TCRs was determined as follows: single-molecule tracking displacements for various time lags between 20 and 140 ms were fitted by a biexponential distribution function (Methods, “TOCCSL analysis”), yielding the fraction of immobile/slowly diffusing TCRs (left; average fraction $f = 0.36 \pm 0.03$), the mean square displacement (msd)–time lag plot of immobile/slowly diffusing TCRs (middle; $D = 0.003 \mu\text{m}^2/\text{s}$) and the msd–time lag plot of fast diffusing TCRs (right; $D = 0.047 \mu\text{m}^2/\text{s}$). The fraction of fast/mobile TCRs is given by $1 - f = 0.64 \pm 0.03$ ($n = 21$ cells). **d**, Anisotropy measurements: T cells were decorated with the indicated probes at saturating conditions for anisotropy measurements as described in the Methods. For each labeling condition, more than 11 cells were used for the analysis. Anisotropy of all four employed fluorescently labeled pMHCs was measured in bilayers decorated with the respective probe ($n = 20$ lipid bilayer regions measured per pMHC labeling variant). **e**, Lactose treatment. T cells were labeled under saturating conditions with AF555-H57-scFv and incubated in imaging buffer, imaging buffer containing 20 mM lactose or imaging buffer containing 20 mM sucrose for 20 min at 4 °C. T cells were then placed onto a lipid bilayer featuring the adhesion molecule ICAM-1. Depending on the carbohydrate pretreatment, FRAP experiments were conducted in the presence of imaging buffer ($n = 21$ cells), imaging buffer containing 2 mM lactose ($n = 16$ cells) or imaging buffer containing 2 mM sucrose ($n = 16$ cells). Mobile fractions for lactose- and sucrose-treated T cells were normalized with regard to the mobile fraction of untreated T cells. **f**, Target binding of employed probes. T cells were exposed to the probes shown at increasing concentrations and their mean fluorescence intensity (MFI) was determined by flow cytometry. MFIs were normalized to those obtained with the highest probe concentration at which probe saturation had occurred (circles). Data were fitted with an exponential function (solid line). Concentrations, at which half of the TCRs were labeled by the respective probes, yielded $1.83 \mu\text{g}/\text{ml}$, $3.5 \mu\text{g}/\text{ml}$ and $27.3 \mu\text{g}/\text{ml}$ for H57-scFv, KT3-scFv and KJ25-Fab, respectively ($n = 10,000$ cells per data point). **g**, Distribution of diffusion coefficients. Single-molecule tracks from **b** were analyzed individually, and for every trajectory the diffusion coefficient was determined by mean square displacement analysis ($n = 1,260$ trajectories). Error bars, s.e.m. (with the exception of **a**, s.d.).



Supplementary Figure 2

Alternative recording mode and channel calibration for dual-color TOCCSL, TCR surface density distribution measured with KJ25-Fabs and single-molecule FRET events in dual-color TOCCSL measurements

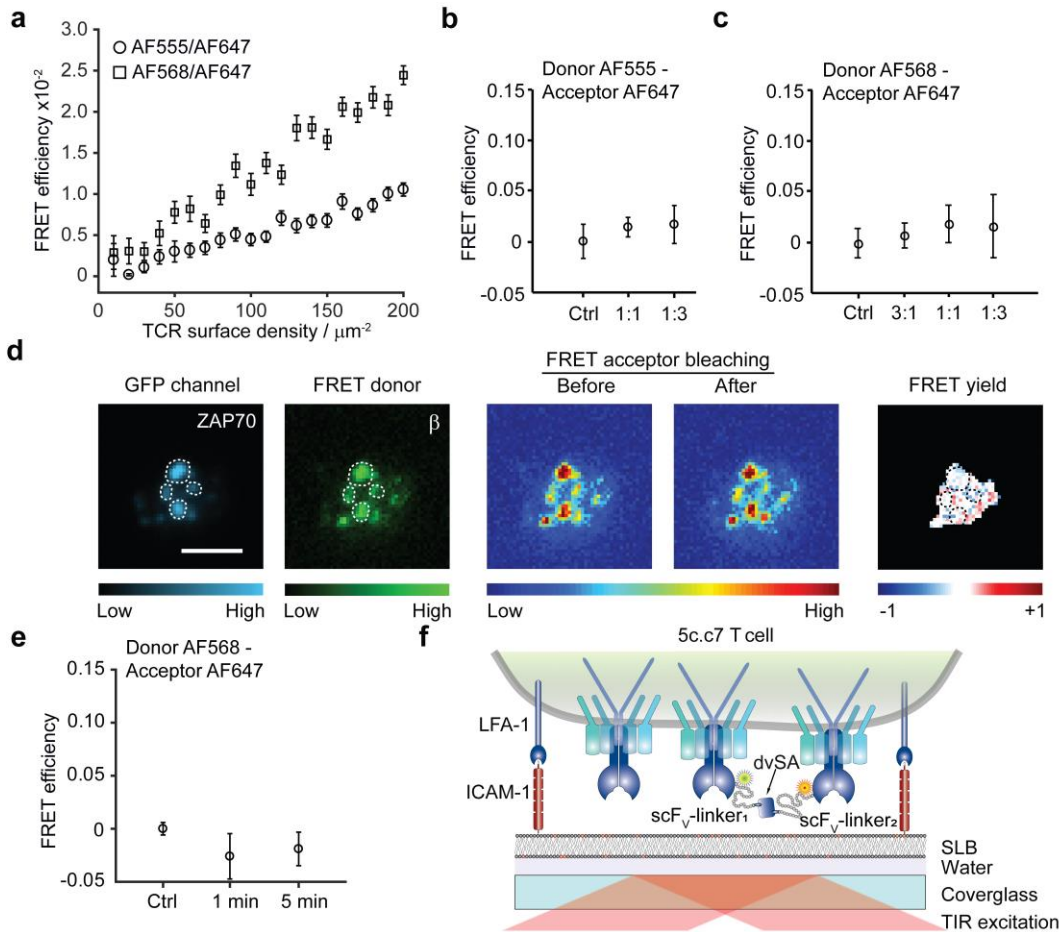
a, Alternative recording mode involving a dual-color TOCCSL image sequence using alternating red and green excitation (shown is a representative experiment). This imaging modality allows not only for dual-color-based colocalization analysis in the TOCCSL image (images i and ii) but may also provide direct evidence of molecular proximities via FRET upon exciting the FRET donor and imaging the FRET acceptor channel (image iii). The dashed area shows the position of the field stop. **b–d**, Channel calibration for dual-color TOCCSL experiments. **b**, Left, the positions of fluorescent multicolor beads detected in the red and green emission channels were overlaid without correction. Right, using this information to calculate the relative shift and stretch of one of the two color channels with respect to the other, the positions of the green color channel were corrected and overlaid with the positions of beads in the red channel. **c**, Histograms of the positional accuracies (PA) of bead positions in the respective channel are shown. The virtual distance of beads after correction (**b**, right) is shown to the right and yields an average value of about 20 nm. **d**, Shown is an example of the distribution of virtual distances for the dual-color TOCCSL experiment with H57-scfV and KJ25-Fab shown in Fig. 2. **e**, TCR surface densities as measured with KJ25-Fabs. An alternative epitope present on the 5C.C7 TCR β chain, which is involved in pMHC binding, is probed with the use of KJ25-Fabs. T cells were labeled with AF488-KJ25-Fab and AF647-KJ25-Fab in a 1:1 ratio and placed on a lipid bilayer featuring ICAM-1. The surface densities were calculated for both probes as described in Fig. 1a, yielding an overall TCR surface density of 76 ± 16 molecules per μm^2 . **f**, Dual-color TOCCSL analysis combined with single-molecule FRET analysis to score for molecular proximity. T cells were simultaneously decorated with AF647-H57-scfV and AF488-KJ25-Fab, and a dual-color colocalization-based TOCCSL experiment was performed. The images were recorded 10 s after the bleach pulse. Positions of diffraction-limited spots were determined for both color channels and are marked with red open circles in the red AF647-H57-scfV channel (top left, red excitation), green open circles in the AF488-KJ25-Fab channel (bottom left, green excitation) and yellow circles in the FRET image (top right, green excitation). Corrected positions of colocalized probes projected into the other color channels are shown as green, red and yellow crosses. For coincidence analysis, the region of interest (ROI) was chosen to ensure the presence of only detection-limited signals (dotted line). Shown is one colocalization (yellow arrow), which is further supported by the presence of a FRET signal (a representative experiment is shown). Scale bars, 4 μm .



Supplementary Figure 3

Autocorrelation functions measured for employed antibody probes in solution

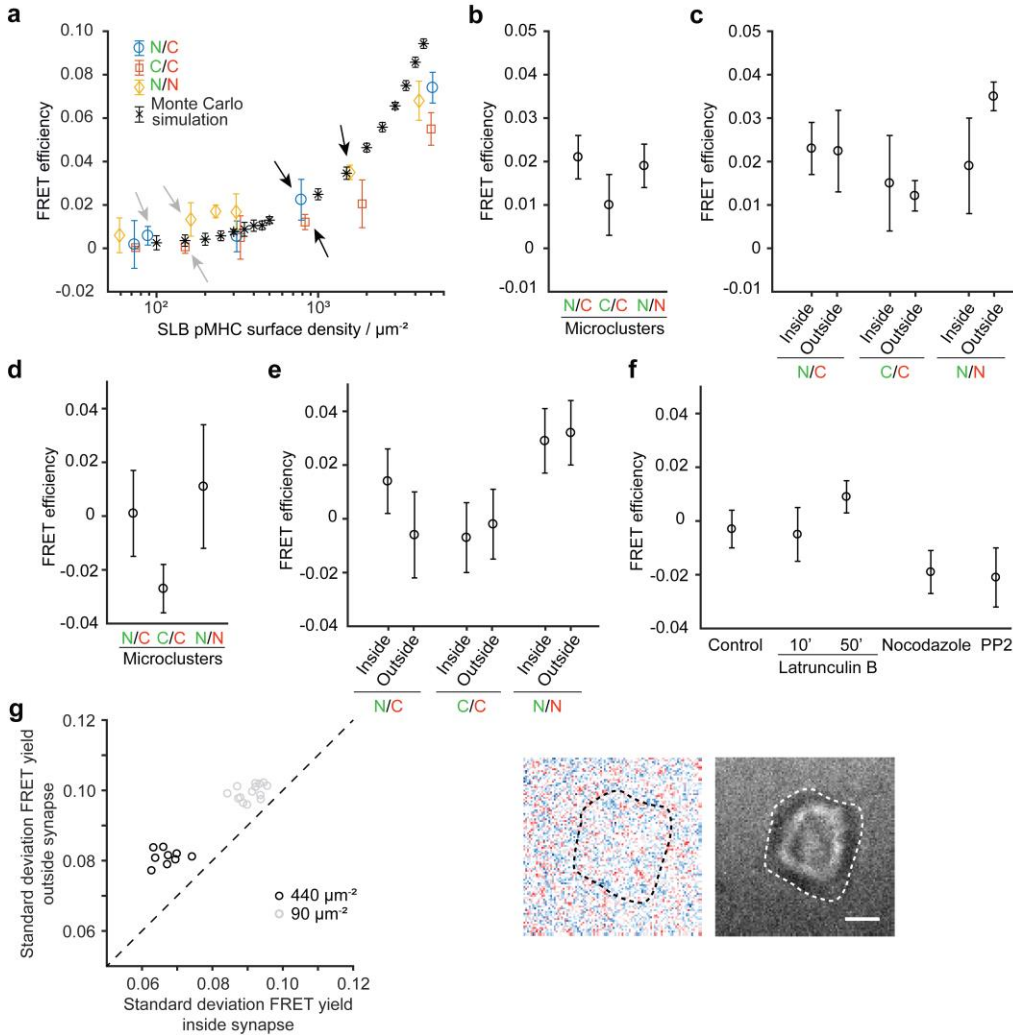
a–c, The left panel shows the measured autocorrelation functions (ACFs) (blue line) of AS635-H57-scFv (**a**), AS635-KJ25-Fab (**b**) and AS635-KT3-scFv (**c**) in solution at a concentration of 1 to 10 nM. The curves were fitted by a 3D diffusion function with one triplet state (red dashed line). In the right panel, ACFs are displayed at 0 s (blue), at the first period (100 ns for H57-scFv and 400 ns for KJ25-Fab and KT3-scFv) (green) and 2 s (red) lag time. Fitting (red and blue lines) yielded an average value of 1.22 ± 0.014 emitters per AS635-H57-scFv molecule ($n = 10$ measurements), 1.26 ± 0.01 emitters per AS635-KJ25-Fab ($n = 12$ measurements) and 1.13 ± 0.01 emitters per AS635-KT3-scFv ($n = 11$ measurements).



Supplementary Figure 5

FRET measured between TCR-bound H57-scFvs

a, FRET values expected from randomized molecular encounters via Monte Carlo simulations are shown at indicated TCR densities (AF555:AF647 = 1:1; AF568:AF647 = 1:1) ($n = 20$ simulations per data point). **b**, FRET efficiencies measured under non-activating (NA) conditions. T cells were labeled with the indicated FRET donor:FRET acceptor ratios (AF555-H57-scFv:AF647-H57-scFv) and placed onto lipid bilayers featuring ICAM-1 and B7-1. Donor recovery after acceptor photobleaching experiments was carried out to determine the ensemble FRET yield. To account for photobleaching, experiments were conducted with green excitation only, and the laser power was adjusted to keep photobleaching below 2% ($n = 11$ cells). FRET could not be detected ($n = 13$ cells), even in the more sensitive experiment involving a 1:3 FRET donor:FRET acceptor labeling ratio ($n = 10$ cells). **c**, Increasing the sensitivity of the FRET-based assay toward longer distances. FRET efficiencies were measured for the AF568:AF647 dye pair exhibiting a larger Förster radius (8.2 nm instead of 5.1 nm). T cells were labeled with different FRET donor:FRET acceptor ratios (AF568-H57-scFv:AF647-H57-scFv) and placed on lipid bilayers featuring ICAM-1 and B7-1 (control, $n = 15$ cells; 3:1, $n = 13$ cells; 1:1, $n = 16$ cells; 1:3, $n = 12$ cells). **d**, Monitoring FRET between TCR-bound H57-scFvs at sites of synaptic ZAP70-GFP recruitment indicative of initial TCR engagement and TCR-proximal signaling. Shown are ZAP70-GFP (blue) and FRET donor (green), as well as FRET donor intensities in false color representation before and after FRET acceptor ablation, which were then used to assay FRET yields during immediate T cell ligand recognition (shown is a representative synapse). For FRET quantification (Methods), brightness values were averaged for sites of local synaptic ZAP70-GFP recruitment representing hotspots of TCR-proximal signaling (dashed lines). **e**, FRET efficiencies at sites of local synaptic ZAP70-GFP recruitment. T cells were labeled with AF568-H57-scFv and AF647-H57-scFv at a ratio of 1:3 and placed onto lipid bilayers featuring ICAM-1, B7-1 and I-E^k/MCC. Donor recovery after acceptor photobleaching experiments was conducted to determine ensemble FRET yields in ZAP70-positive TCR microclusters at first contact of T cells with lipid bilayers (<1 min) or at a later time point (5 min) (control, $n = 11$ cells; 1 min, $n = 13$ cells, 28 microclusters; 5 min, $n = 17$ cells, 40 microclusters). **f**, Rationale underlying the FRET-positive control. T cells were labeled with biotinylated H57-scFv probes (scFv-linker1-AF555 and scFv-linker2-AF647) at a ratio of 1:1. After cross-linking probes by applying different concentrations of streptavidin, which was engineered to feature only two (instead of four) biotin-binding sites positioned in trans, T cells were placed onto lipid bilayers containing ICAM-1 and B7-1. Scale bars, 3 μm . Error bars, s.e.m.



Supplementary Figure 6

FRET measured between site-specifically labeled bilayer-resident pMHCs

a–c, FRET efficiencies measured on lipid bilayers featuring pMHC FRET pairs. **a**, Lipid bilayers were charged with the indicated combinations of I-E^k/MCC-AF555(N), I-E^k/MCC-AF555(C), I-E^k/MCC-AF647(N) and I-E^k/MCC-AF647(C) at densities amounting to up to 5,000 pMHCs per μm^2 ($n = 10$ regions measured on lipid bilayer per density, $n = 20$ simulations per data point). Black arrows specify lipid bilayer samples with which T cells had been confronted for determination of inter-pMHC FRET yields at high surface densities, and gray arrows indicate inter-pMHC FRET measurements at 37 °C. **b,c**, FRET efficiencies at high pMHC surface densities as determined within individual TCR microclusters (N/C, $n = 18$ cells, 88 microclusters; C/C, $n = 13$ cells, 83 microclusters; N/N, $n = 14$ cells, 79 microclusters) (**b**) and entire synapses (N/C, $n = 18$ cells; C/C, $n = 13$ cells; N/N, $n = 14$ cells) (**c**). **d,e**, FRET efficiencies were determined at 37 °C within individual TCR microclusters (N/C, $n = 22$ cells, 83 microclusters; C/C, $n = 11$ cells, 124 microclusters; N/N, $n = 15$ cells, 92 microclusters) (**d**) and entire synapses (N/C, $n = 22$ cells; C/C, $n = 11$ cells; N/N, $n = 15$ cells) (**e**). **f**, FRET efficiencies were measured on lipid bilayers featuring I-E^k/MCC-AF555(N) and I-E^k/MCC-AF647(C) in TCR microclusters after treatment with pharmacological inhibitors. FRET yields were determined before treatment (control, $n = 11$ cells, 49 microclusters), 10 or 50 min after addition of 10 μM latrunculin B (10 min, $n = 12$ cells, 56 microclusters; 50 min, $n = 11$ cells, 30 microclusters) and 55 min after addition of 100 μM nocodazole ($n = 15$ cells, 76 microclusters). For p56^{lck} kinase inhibition, T cells were pretreated for 60 min with 10 μM PP2 and FRET yields were determined after microcluster formation ($n = 11$ cells, 32 microclusters). **g**, Heterogeneity of inter-I-E^k-FRET yields in synapses of mismatched OT-1 TCR-transgenic T cells. The s.d. values of pixel-wise FRET yields within the synapse were correlated to corresponding s.d. values measured outside the synapse at two different bilayer densities (left; 90 μm^{-2} , $n = 9$ cells; 440 μm^{-2} , $n = 14$ cells). A representative experiment involving an OT-1 TCR-transgenic T cell confronted with a bilayer featuring ICAM-1, B7-1 and I-E^k/MCC-AF555(N) and mismatched I-E^k/MCC-AF647(C) with visualized pixel-wise FRET yields is shown on the right. Scale bars, 3 μm . Error bars, s.e.m.

Supplementary table 1. Förster radii R_0 for used Alexa dye pairs (values from ThermoFisher)

Donor dye	Acceptor dye	R_0 in angstroms (Å)
Alexa Fluor 488	Alexa Fluor 647	56
Alexa Fluor 555		51
Alexa Fluor 568		82